

# Chapter 304

## A Thermal Comfort Modelling Framework for Urban Neighbourhoods: Tempo-Spatial Coupling of Building Energy and CFD Models



Reihaneh Aghamolaei, Marzieh Fallahpour, Ruijun Zhang,  
and Parham A. Mirzaei

**Abstract** More accurate tools are required to replicate urban climates to achieve healthy and comfortable urban environments. To this end, this study implements a novel high-resolution simulation framework to improve the OTC modelling by dynamic coupling of convective fluxes calculated by computational fluid dynamic (CFD) model, and dynamic building energy simulation (BES) for analyzing outdoor surface temperature of buildings. In addition, radiative fluxes emitted from building surfaces are coupled with latter models. The workflow is applied at the Grasshopper platform based on the results of ANSYS Fluent as the CFD and EnergyPlus as the BES tools. This framework is tested within a generic case study representing an urban neighbourhood. As a result of this framework, tempo-spatial values for OTC are achieved at each time-step of simulation and then compared with the OTC values from the traditional OTC modelling approach. Statistical analysis of results shows that the OTC valued predicted using the coupled method can change considerably compared to OTC results from traditional methods at the neighbourhood scale.

**Keywords** Outdoor thermal comfort · Tempo-spatial · Computational fluid dynamics · Building energy simulation

---

R. Aghamolaei  
School of Mechanical and Manufacturing Engineering, Faculty of Engineering and Computing,  
Dublin City University, Whitehall, Dublin 9, Ireland

M. Fallahpour  
College of Fine Arts, University of Tehran, Tehran, Iran

R. Zhang · P. A. Mirzaei (✉)  
Architecture and Built Environment Department, University of Nottingham, University Park,  
Nottingham NG2RD, UK  
e-mail: [Parham.Mirzaei\\_ahranjani@Nottingham.ac.uk](mailto:Parham.Mirzaei_ahranjani@Nottingham.ac.uk)

### 304.1 Introduction

One of the most important effects of fast-growing urbanization is reducing outdoor thermal comfort (OTC) which can endanger the health of people living in urban areas and increase the outdoor surface temperature of building envelopes and, as such, intensifies the cooling load and electricity consumption of surrounding buildings (Li et al. 2018; Mirzaei and Haghighat 2010). OTC is a main measure for public space design and quality assessment to improve the performance of the outdoor built environment (Shooshtarian and Ridley 2017), which is critical for site attractiveness, people's outdoor activities, and overall quality of life (Peng et al. Jan. 2019). To Investigate OTC, a wide verity of studies has been carried out with local field measurements or numerical simulations. Although field measurements provide valuable and realistic results, computational models are considered to be faster and applicable to large urban scales (Deng and Wong 2020; Aghamolaei et al. 2020).

OTC models encounter more difficulties and complexities compared to those implemented for indoor thermal comfort modelling. In OTC modelling, radiative and convective fluxes are found to be the most significant factors that increase the complexity of the modelling process. In this regard, several tools are utilized to calculate OTC such as RayMan, SOLWEIG, SkyHelios, ENVI-met, Ladybug-Grasshopper plugins, and tools based on computational fluid dynamics (CFD) analysis such as Autodesk CFD and AnsysFluent (Aghamolaei et al. 2021). ENVI-met and Rayman are as the most commonly used simulation tools to calculate the thermal comfort performance of urban areas. The mean radiant temperature of large-scale urban areas is also studied with radiation-based models such as Solar and LongWave Environmental Irradiance Geometry (SOLWEIG). As this tool applies static approaches to analyse the 3D radiant flux densities without considering the convective fluxes and urban airflow, results in simplifying the effect of wind velocity in open spaces (Lindberg et al. 2008). Tominaga and Stathopoulos (2013) assessed the effects of the density of different building layouts on OTC results by Rayman tool. In a more recent study, the interaction of temperature of building envelopes with pedestrian thermal comfort was investigated using Honeybee and Ladybug plugins within Grasshopper environment (Aghamolaei et al. 2021; Evola et al. 2020).

Microclimate CFD models are more focused on the solution of convective fluxes, contrary to radiation-based tools, and have been also widely employed for analysing pedestrian-level thermal comfort in urban areas. Microclimate CFD models can provide convective fluxes data for any considered variables within the whole computational domain (Moonen et al. 2012). The restricted domain size due to the high CPU cost, the huge computational cost of microclimate radiation calculation, and not including the atmospheric phenomena are the limitations of microclimate CFD simulation (Mirzaei and Haghighat 2010). Also, both radiation-based and microclimate CFD tools are unable to cover the dynamic response of buildings in terms of radiative and convective fluxes which coupling CFD and radiation-based models is a solution for that (Khoshdel Nikkho et al. 2017).

The above literature review highlights different OTC computation models and tools. It also reveals that most thermal comfort studies focused on one of the radiative or convective models. Moreover, an accurate investigation of the thermal interaction of building envelopes (surface temperature) plays an important role in the OTC calculation process. However, a few numbers of studies included all these three models of radiation, airflow and surface temperature into the OTC modelling procedure.

The present paper presents a novel simulation framework to improve OTC modelling in urban areas. This research develops a high-resolution framework to couple radiative and convective fluxes in outdoor spaces (using CFD) with building surface temperatures calculated by envelope building energy simulation (BES) approaches. The proposed methodology develops a generalisable framework that is applicable to different locations and design scenarios. The applicability of this framework is examined by using a general case study in the city of Tehran. In this paper, Sect. 304.2 highlights the methodology to develop the CFD analysis and OTC modelling framework. Section 304.3 outlines the results and discussions of this OTC modelling framework and explains the settings required to apply in the case study, and, Sect. 304.4 summarizes the conclusions and suggestions for future research.

### 304.2 Novel Framework

This framework is based on a step-by-step process to enhance the OTC modelling in urban areas including 3 modules: (1) surface temperature of building envelopes calculated based on the energy modelling of buildings, (2) air velocity values calculated by CFD study, (3) radiative fluxes analysed and then coupled by imported results from step 1 and 2 to calculate the OTC results. The used tools for each module are EnergyPlus for energy modelling of buildings, ANSYS Fluent to analyse the air velocity values and finally, Honeybee plugin of Grasshopper to calculate both radiative results and OTC values (Fig. 304.1).

In order to find the impact of wind velocity values in the performance of the OTC model, a T-test and sensitivity analysis were performed for all points at different times

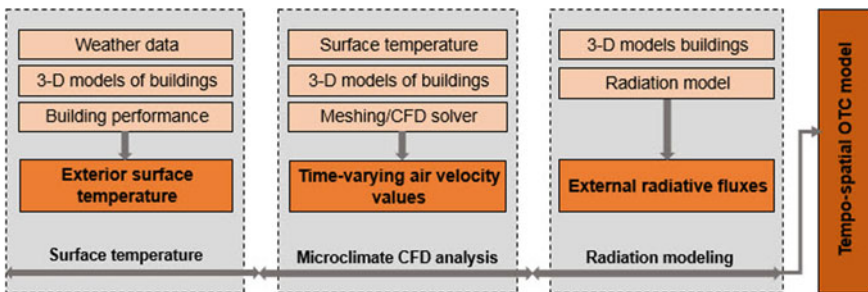


Fig. 304.1 The overarching diagram of the OTC modelling framework

of a day. The tempo-spatial distribution of physiological equivalent temperature (PET) is compared in two different scenarios, including (1) using constant wind values for all simulation points as a traditional approach, and (2) using microclimate CFD results for wind values at all simulation points. The effect of applying CFD results in OTC models for each sample was calculated as the function of the equation below which standardized the impact of applying this framework on the OTC results.

$$SI_h = \left| \frac{OTC_2 - OTC_1}{OTC_1} \right| \times 100 \quad (304.1)$$

where  $SI_h$  is standardized impact at a specific time,  $h$  is the hour of simulation,  $OTC_2$  is the simulated PET value in scenario two (OTC based on microclimate CFD results) and  $OTC_1$  is the simulated PET value for scenario one (OTC based on constant wind values).

### 304.2.1 Methodology

#### 304.2.1.1 Energy Performance and Surface Temperature

To investigate the application of this framework, a general building complex including nine 7-story residential buildings was selected (Fig. 304.2). Then, the outdoor surface temperatures of building envelopes were simulated via EnergyPlus. For conducting the energy analysis, 63 thermal zones were defined each showing one floor of these nine buildings. As this framework captures the temporal and spatial variation of OTC in urban areas, a complete day was selected to conduct the simulations (8:00–19:00 on May 22nd). The wind rose of Tehran as the case study of this research was simplified to 20 wind scenarios after stochastic analysis to understand more probable wind directions and magnitudes for Tehran climate as represented in Table 304.1.

**Fig. 304.2** a Schematic of the selected case study and b mesh configuration of the case study

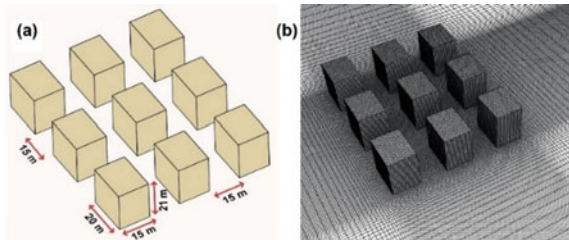


**Table 304.1** Wind scenarios for the CFD model

Wind velocity (m/s)	Wind direction
0.8	90–135
2	180–225–315
3	45–90–270
5.2	0–315
8.1	0–180–270–315
11.6	45–225–315
13.5	0–180–270

**304.2.1.2 Microclimate CFD Simulation**

3D steady Reynolds-Averaged Naviere Stokes (RANS) CFD simulations were performed to simulate the wind velocity of the microclimate case study with regard to real-time buildings surface temperature. Geometry was created in the ANSYS Design Modeler program and the mesh configuration of the case study was made in the ICEM software as shown in Fig. 2a and b, respectively. A grid sensitivity study was conducted with a coarser and a finer grid resulted in the 3% deviation between the finer and basic mesh. It could be concluded that the 0.75 m hexahedral grid with a cell count of 28 per building height and 20 per canyon width was appropriate for reliably microclimate CFD simulation. ANSYS Fluent as the CFD software was utilized to evaluate a three-dimensional numerical model. Boundary conditions and solver settings for the microclimate CFD simulation reported in Table 304.2.

The microclimate CFD model was validated against measurements from an experimental wind tunnel study by AIJ-case C (Tominaga et al. 2008) with two strategies,

**Table 304.2** Boundary conditions and solution schemes of the microclimate CFD model

Parameter	Value
Inflow boundary	$U(z) = \frac{u_*}{k} \ln\left(\frac{z+z_0}{z_0}\right), k(z) = \frac{u_*^2}{\sqrt{c_\mu}}, \varepsilon(z) = \frac{u_*^3}{k(z+z_0)}$
Outflow boundary	Zero static pressure
Ground boundary	Logarithmic law with roughness length of $k_s = 0.3$ m and $C_s = 1$
Upper and side surface of domain	Symmetry condition
Building surface boundary	Logarithmic law with roughness length of $k_s = 0.1$ m and $C_s = 0.5$ a user-defined function file for the surface temperature of buildings
Turbulent scheme	Realizable k- $\varepsilon$
Momentum discretization	Second-order upwind
Computational domain	$L = 495$ m $\times$ $W = 300$ m $\times$ $H = 105$ m
Hexahedral cells number	2,034,396

$z_0 = 0.03$  m,  $\kappa = 0.40, u^* = 0.25$  m/s  $c_\mu = 0.09$

including wind tunnel (scaled) size and real-size (75 times the scaled-size) models with the length of the first layer cell ( $x$ ) of 0.01 m and 0.75 m (same size of case study mesh), respectively, in order to maintain the grid consistency and comparability, that both corresponded with the cell counts of 20 along with the building height.

### **304.2.1.3 Calculation of Comfort Model**

The coordinates and velocity results of all points were imported from the microclimate CFD study to the Rhinoceros 3D<sup>®</sup> environment via “.csv” files to analyse the OTC for all of them at a height of 1.5 m. Also, the results from the energy model (surface temperatures) were imported to the OTC model for each point to produce the tempo-spatial OTC performance report.

In this study, PET is used as the default OTC index for determining the acceptable comfort range. PET as a commonly-used thermal comfort index incorporates the effects of air temperature, relative, humidity wind speed and MRT into account (Galindo and Hermida 2018; Shih et al. 2017). PET is based on the Munich Energy-balance Model for Individuals (MEMI), which models the thermal conditions of the human body in a physiologically relevant way (Höppe 1999; Matzarakis and Amelung 2008). MEMI collects all the meteo-climatic and human activity data into a single temperature index of PET. In compared to other OTC models, PET is more used as it easier to understand since it represents the temperature for measuring OTC. It is also adopted specifically for outdoor areas where thermal discomfort can be high (Walther and Goestchel 2018).

### **304.2.2 Case Study City**

Simulations were carried out in a selected case study in the city of Tehran. The city is selected because of harsh solar radiation and considerable wind velocity pattern. Tehran has longitude 51° 19' E and latitude of 35° 41' N with the elevation of 1190 m. In BSk Köppen climate categorization system, Tehran has a mid-latitude steppe and semi-arid cool climate (Weather 2017).

## **304.3 Results and Discussion**

### **304.3.1 Microclimate CFD Validation Results**

Figure 304.3 compares the wind velocity of microclimate CFD simulations for the scaled-size model, at 0.02 m above ground and for the real-size model, at 1.5 m above ground that both were normalized by the approach flow velocity at the building's

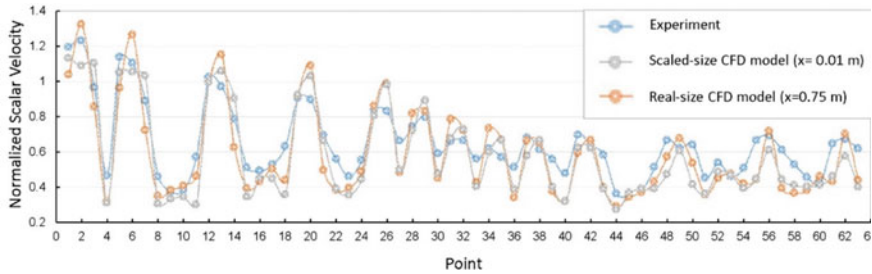


**Fig. 304.3** Comparison of measured and simulated wind speeds at 0.02 m above ground for scaled-size model and at 1.5 m above ground for the real-size model

height at all points with the wind tunnel measurement results. Average deviations of 17.23% and 17.67% are achieved between the scaled- and real-size model simulations with the experimental results, respectively.

### 304.3.2 OTC Modelling

The proposed modelling framework is used to investigate the tempo-spatial distribution of OTC in urban areas. The results of the T-test show that there is a significant change in the OTC results after applying the CFD values in the calculation process (Table 304.3). As it is shown in Table 304.3, the P values for all the wind scenarios are less than 0.05 which confirms that the results of the T-test are significant.

Figure 304.4 highlights the sensitivity of the OTC model for applying CFD results in the calculation process (see Eq. 304.1). When the air velocity is 0.8 m/s at 8:00, about 35% of points experience 5–7% changes in the PET values (SI of 5–7%). Also, a higher rate of changes in PET values was observed, for instance, 1% of all points have experienced 18.75% changes at this time of the day (Fig. 304.4a). When air velocity increases to 8.0 m/s at 13:00 (Fig. 304.4b), the SI values also increases accordingly. For instance, about 55% of points experienced more than 20% changes in the PET values. In this condition, PET results are also changed for about 48–54% at 1% of all points of the case. A similar pattern is also observed at wind velocity of 13.5 m/s, in which 24% of selected areas, experience 20–24% changes in the OTC results after applying accurate CFD results at 12:00 (Fig. 304.4c).

In terms of the distribution of changes in the temporal dimension, the results of two scenarios of OTC modelling (with constant wind velocity and coupling with CFD results), are depicted in Fig. 304.5 at 3 h of a day by means of box and whisker diagram that plots the distribution pattern of numeric data. As depicted in Fig. 304.5, the total trend of OTC results is quite consistent in these two scenarios. However, comparing the length of quantiles shows that OTC results in scenario-2 with CFD-driven values are distributed in a wider range. For example, in Fig. 304.5b, the PET values of scenario-1 are within the range of 26–43 °C while, in scenario-2, these



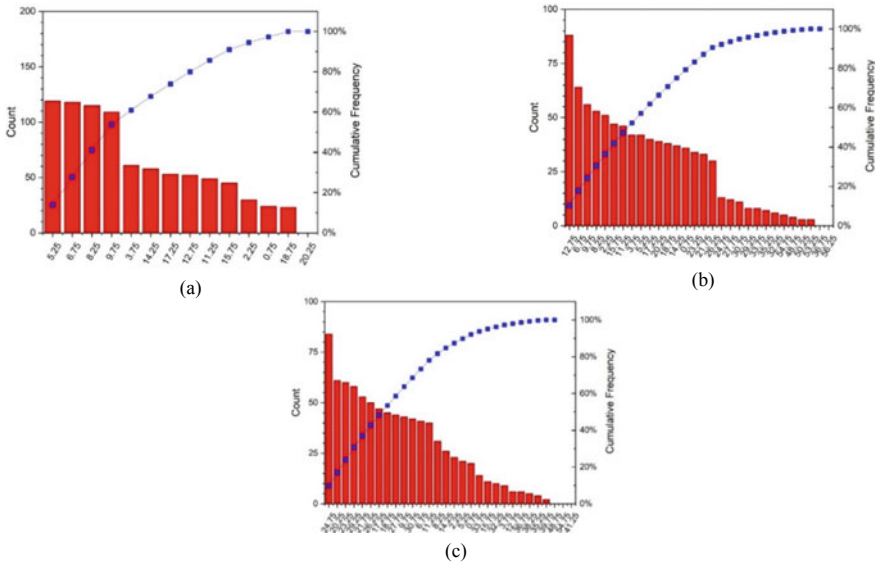


**Fig. 304.4** This diagram shows the SI value for the results of OTC models highlighting the effect of applying CFD results in OTC values: **a** wind velocity of 0.8 m/s at 8:00, **b** wind velocity of 8.0 m/s at 13:00, **c** wind velocity 13.5 m/s at 12:00

values are varying from 25 to 50 °C. Similarly, in Fig. 304.5c, the PET values start from 26 to 41 °C in scenario-1 while in scenario-2 the upper limit rises up to 48 °C. Also, Fig. 304.5 shows that each point experiences a wider range of PET when CFD-based results are incorporated while, by using constant wind values, this wide range of PET values is not seen.

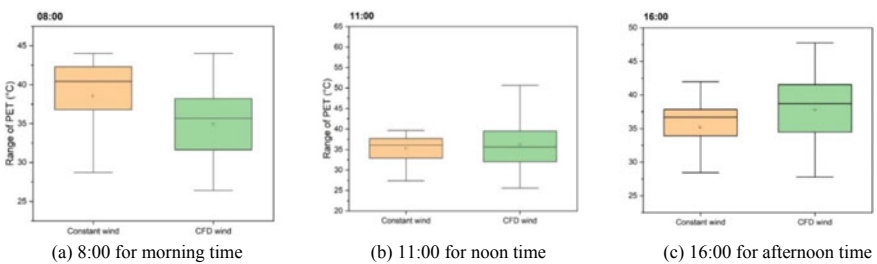


**Fig. 304.5** Calculated PET values of each point for two different scenarios: (1) constant wind values, and (2) CFD simulated wind conditions

### 304.4 Conclusion

This study developed a comprehensive framework for improving OTC modelling in built-up areas by integrating solar radiation (radiative fluxes), airflow model (convective fluxes by CFD analysis) and envelopes' surface temperature (energy analysis). The results provide novel insights into tempo-spatial OTC performance modelling at the pedestrian level and also highlights the critical areas during different hours of a day. The main concluding points of this paper are:

- The tempo-spatial modelling process of OTC at neighbourhood scales is improved with this framework without increasing the computation cost of the coupling procedures.
- Results show that each point experiences a wider range of PET values when CFD-based results are incorporated while, by using constant wind values, this wide range of PET values didn't happen.
- Coupling microclimate CFD and OTC models significantly changes the OTC results. Results show that about 40% of points experienced more than 10% changes in the calculated PET values at 8:00, while, at 13:00, about 55% of points experienced more than 20% changes in the PET values, and also, 8% of the total area had more than 30% changes in PET values at 12:00.
- By coupling CFD and OTC models, the most changes of the PET values happened at the building's edges and in areas close to building surfaces that also make considerable tension in the wind profile causing local discomfort for pedestrians.

This study formulates a generic framework that is not location/design scenario specific. Futures studies can investigate the impact of the integration of such frameworks in relation to the geometry of buildings to help the architects and planners to understand the impact of their design scenarios.

### References

- Aghamolaei R, Azizi MM, Aminzadeh B, Mirzaei PA (2020) A tempo-spatial modelling framework to assess outdoor thermal comfort of complex urban neighbourhoods. *Urban Clim* 33:100665. <https://doi.org/10.1016/j.uclim.2020.100665>
- Aghamolaei R, Fallahpour M, Mirzaei PA (2021) Tempo-spatial thermal comfort analysis of urban heat island with coupling of CFD and building energy simulation. *Energy Build* 111317
- Deng J-Y, Wong NH (2020) Impact of urban canyon geometries on outdoor thermal comfort in central business districts. *Sustain Cities Soc* 53:101966
- Evola G, Costanzo V, Magri C, Margani G, Marletta L, Naboni E (2020) A novel comprehensive workflow for modelling outdoor thermal comfort and energy demand in urban canyons: results and critical issues. *Energy Build* 109946
- Galindo T, Hermida MA (2018) Effects of thermophysiological and non-thermal factors on outdoor thermal perceptions: the Tomebamba Riverbanks case. *Build Environ* 138(April):235–249. <https://doi.org/10.1016/j.buildenv.2018.04.024>
- Höppe P (1999) The physiological equivalent temperature—a universal index for the biometeorological assessment of the thermal environment. *Int J Biometeorol* 43(2):71–75

- Khoshdel Nikkho S, Heidarinejad M, Liu J, Srebric J (2017) Quantifying the impact of urban wind sheltering on the building energy consumption. *Appl Therm Eng* 116:850–865. <https://doi.org/10.1016/j.applthermaleng.2017.01.044>
- Li G, Zhang X, Mirzaei PA, Zhang J, Zhao Z (2018) Urban heat island effect of a typical valley city in China: responds to the global warming and rapid urbanization. *Sustain Cities Soc* 38:736–745
- Lindberg F, Holmer B, Thorsson S (2008) SOLWEIG 1.0—modelling spatial variations of 3D radiant fluxes and mean radiant temperature in complex urban settings. *Int J Biometeorol* 52(7):697–713
- Matzarakis A, Amelung B (2008) Physiological equivalent temperature as indicator for impacts of climate change on thermal comfort of humans. In: *Seasonal forecasts, climatic change and human health*. Springer, pp 161–172
- Mirzaei PA, Haghighat F (2010) Approaches to study urban heat island e abilities and limitations. 45:2192–2201. <https://doi.org/10.1016/j.buildenv.2010.04.001>
- Moonen P, Defraeye T, Dorer V, Blocken B, Carmeliet J (2012) Urban physics: effect of the microclimate on comfort, health and energy demand. *Front Archit Res* 1(3):197–228. <https://doi.org/10.1016/j.foar.2012.05.002>
- Peng Y, Feng T, Timmermans H (2019) A path analysis of outdoor comfort in urban public spaces. *Build Environ* 148:459–467. <https://doi.org/10.1016/j.buildenv.2018.11.023>
- Shih W-M, Lin T-P, Tan N-X, Liu M-H (2017) Long-term perceptions of outdoor thermal environments in an elementary school in a hot-humid climate. *Int J Biometeorol* 61(9):1657–1666
- Shooshtarian S, Ridley I (2017) The effect of physical and psychological environments on the users thermal perceptions of educational urban precincts. *Build Environ* 115:182–198
- Tominaga Y et al (2008) AIJ guidelines for practical applications of CFD to pedestrian wind environment around buildings. *J Wind Eng Ind Aerodyn* 96(10–11):1749–1761
- Tominaga Y, Stathopoulos T (2013) CFD simulation of near-field pollutant dispersion in the urban environment: a review of current modeling techniques. *Atmos Environ* 79:716–730. <https://doi.org/10.1016/j.atmosenv.2013.07.028>
- Walther E, Goetschel Q (2018) The PET comfort index: questioning the model. *Build Environ* 137:1–10
- Weather (2017) Weather data by location|EnergyPlus